Student ID: 1918110

University of Birmingham

Course: Brain Imaging and Cognitive Neuroscience MSc

Assessment: Research Report

Simultaneous EEG and fMRI

Practical tutor's name: Dr Stephen Mayhew

Word counts: 1999

1. ELECTROENCEPHALOGRAPHY - EEG

To measure the electrical activity of the brain, one of the most popular methods is EEG. Neuronal activity is recorded by placing electrically conductive metal (Ag/AgCl) electrodes indirectly on the scalp (Cohen, 2017). The detected signal is generated by comparable changes in the electric potentials of the neuronal cells' membrane that is added-up and results in synchronous neuronal activity (Babiloni et al., 2009). Only active firing neuronal populations that are spatially and geometrically aligned are detectable by EEG scalp electrode recording. The main recorded sources of the EEG signal are post-synaptic potentials, produced by the cortical pyramidal cells that are perpendicular to the cortical surface and organised in columns (M. Teplan, 2002).

EEG provides information directly and non-invasively about the electrical activity of the brain with an excellent temporal resolution scale. This feature allows a continuous observation of the dynamic changes of the neuronal activity. Small and quick alternations in the electrical activity can be captured just after the stimulus (Cohen, 2017).

The elementary limitation of EEG arises from different conductivities of the anatomical layers of the head resulting the weakened electrical signal and limited localisation of the neuronal generators (Babiloni et al., 2009; Ruff & Huettel, 2014).

2. FUNCTIONAL MAGNETIC RESONANCE IMAGING - fMRI

Presently, fMRI is the dominant imaging technique in cognitive neuroscience. The imaging procedure is an additional protocol of magnetic resonance imaging (MRI). Image acquisition in fMRI follows the same principles as traditional MRI; the application of (a) a strong main magnetic field (B_0), (b) radio frequency pulses (RFP) and (c) gradient magnetic fields. These are generated by three crucial elements of the MRI hardware (a) a main magnetic coil (supercooled), (b) radiofrequency coils and (c) gradient coils (Currie et al., 2012).

(a) The main magnetic coil generates a constant, strong magnetic field and affects the hydrogen nuclei to align in parallel or antiparallel with the direction of B_0.

(b) The radiofrequency coil transmits RFP to excite the atomic nuclei to precess on a certain frequency (Larmor frequency) and absorb the induced radiofrequency signal from the tissue of interest.

(c) The gradient coils are the equivalent to the three dimensions (x, y, z) and are capable of generating spatial gradients in the magnetic field by switching on one of the coils and influencing the magnetic field strength along a particular direction (Ruff & Huettel, 2014).

Blood-oxygen-level-dependent (BOLD) contrast is the type fMRI that is the most frequently used and was firstly described in the late 1980s by Ogawa (Ogawa et al., 1990). BOLD contrast is based on detecting changes in the oxygen concentration and the blood flow in activated brain regions (Logothesis, 2008). At the stimulus onset, the ratio of oxygenated and deoxygenated haemoglobin concentration is unbalanced as the oxygen use in the activated area is increased; resulting in an increase of the deoxygenated haemoglobin (dHB) concentration (Logothesis, 2002.) The paramagnetic property of dHb causes alternation in the magnetic resonance (MR) signal. BOLD can be interpreted as an endogenous marker of brain function as it originates from haemodynamic signals, it is an indirect measure of the neuronal activity and depends on neurovascular coupling (Ruff & Huettel, 2014).

High resolution images can be obtained non-invasively with fMRI as the excellent spatial resolution of it allows to map entire brain on the order of millimetres. The temporal resolution of fMRI is limited due to slow development of the haemodynamic response. The peak of the BOLD responses takes 5-6 seconds to develop. Therefore, the obtained signal is delayed relative to the stimulus onset (Babiloni et al., 2004).

3. SIMULTANEOUS EEG and fMRI

EEG and fMRI are the two most frequently used non-invasive imaging techniques. EEG and fMRI are antagonists with respects to their spatial and temporal resolutions. This inspired a promising approach: the multimodal combination of the two techniques could produce powerful and complementary results with both high spatial and temporal resolutions (Herman & Debener, 2018). Simultaneous acquisition has the potential to present the relationship between electrical brain activity and haemodynamic responses. It is the most efficient integration of EEG and fMRI because of its power to investigate trial-by-trial fluctuations of evoked brain activity from neural generators spatially and temporally identical (Debener et al., 2006).

The primary application of simultaneous recording was focused on non-invasively mapping epileptic networks for seizure localisation in drug-resistant patients (Ives et al., 1993). Although it was firstly used for clinical applications, it has started to dominate the field of cognitive neuroscience more generally. Simultaneous recording is promising: to measure the variability of alpha-BOLD relationships during resting-state and task (Mayhew & Bagshaw, 2017), for epilepsy research as a multimodal tool (Gotman et al., 2006) or for the application of multiband fMRI with simultaneous EEG (Uji et.al, 2018).

Simultaneous acquisition is challenging mainly due to the technical differences in the foundations of each domains. Specific safety issues related to the participants and the equipment have to be taken into consideration. The EEG electrodes and leads are made of conductive materials. The switching pattern of the gradient coils during fMRI data acquisition have an effect on the homogeneity of the magnetic fields. According to Faraday's law, changes in the homogeneity induce a current in the EEG cables. Similarly, any movements of the electrode lead or the participants' head could cause a current and alter the homogeneity of the magnetic field (Lemieux, et al, 1997).

The transmitted RFP during slice acquisition generates energy that is absorbed by the electrode cables and the participants' tissue. This energy then expends as heat close to the electrodes, which could

potentially increase the risk of burning injuries (Laufs et al., 2008). To prevent the possible heating complications and discomfort of the participants; it is recommended to use low specific absorption rate (SAR, *see Appendix 1*) (Mele et al., 2019). SAR measures the potential rate of the absorbed energy of the patient's tissue due to the application of the RFP for image acquisition.

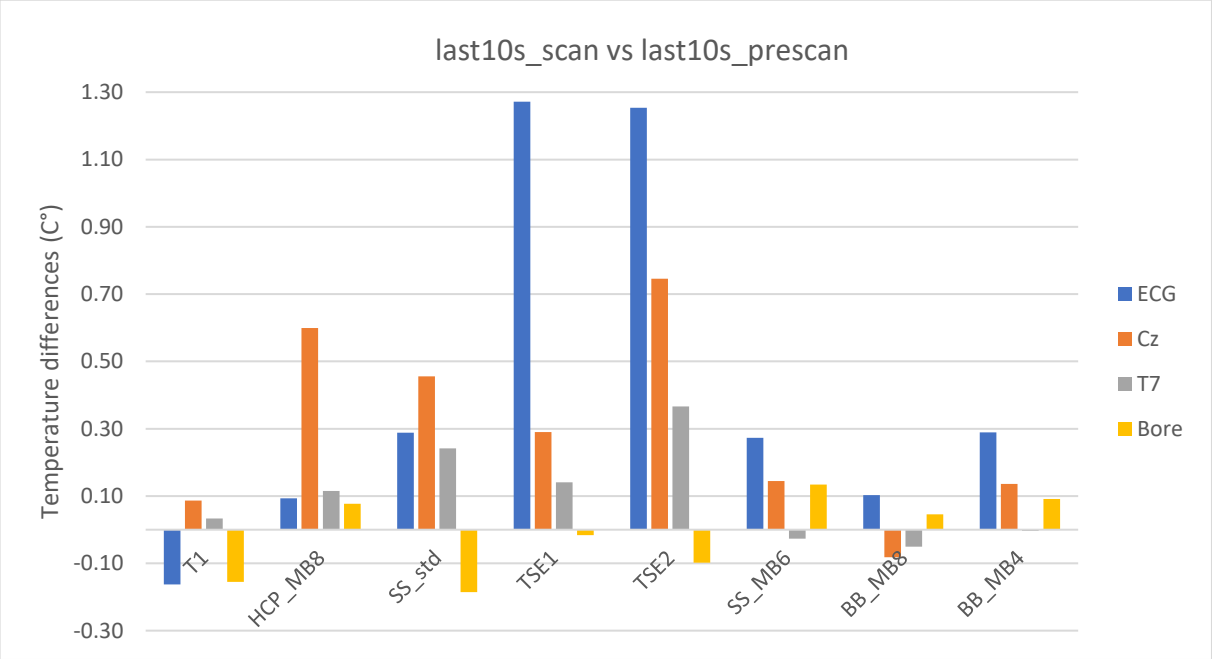

Figure 1. The measured heating changes (in Celsius) during different MR scans on 3 EEG electrodes and the main magnet bore. The x axis represents the anatomical and functional scans, the y axis indicates the temperature changes. The measured temperatures are compared between the last 10 seconds of the given scan and the last 10 seconds of the previous scan. The TSE1 and TSE2 scans induced the most noticeable heating change in the ECG electrode, as it would have been expected due to its much higher SAR rate. Scans that using multiband slice acquisition generated relatively large temperature change on Cz and ECG electrodes.

Table 1. The SAR rate of the used scans

	Scan		SAR rate	
1	T1	T1	11%	0.3 W/kg
2	Human Connectome Project, Multiband 8	HCP_MB8	12%	0.4 W/kg
3	Siemens standard BOLD	SS_std	12%	0.4 W/kg
4	T2 Turbo Spin Echo	TSE1	54%	1.7 W/kg
5	Two runs T2 Turbo Spin Echo	TSE2	54%	1.7 W/kg
6	Siemens Multiband 6	SS_MB6	12%	0.4 W/kg
7	Biobank Multiband 8	BB_MB8	12%	0.3 W/kg
8	Biobank Multiband 4	BB_MB4	12%	0.3 W/kg

Synchronising the clocks of the EEG and the MR system is inevitable to ensure the temporal accuracy of the simultaneous recording. Physical connection is essential; this can be achieved by directly connecting the EEG amplifiers and the MR scanner electronics hardware. The connection must be phase synchronised with the gradient system of the MR hardware (Gebhardt et al., 2008).

The original setups of EEG and MRI scanner are technically not compatible for simultaneous recording; therefore, further modifications are necessary. To date, there are several MRI environment compatible EEG systems available. Currently, there are two different methods for positioning the EEG system: (a) outside or (b) inside the scanner room. Both options have their own advantages and limitations.

(a) *Outside*: The main advantage is that no adjustments are necessary on the current EEG system as the amplifiers are not being affected by the strong magnetic field of the MR hardware. As a result, there is a huge distance between the amplifier and the electrode system resulting in the connecting cables being extremely long. The degree of the induced current in the electrode leads depends on the cable length, thus longer leads means bigger artefacts. Furthermore, the increased cable length could result in a decay in EEG signal (Ullsperger & Debener, 2010).

(b) *Inside*: The length of the leads between the MR environment compatible amplifier and the electrode cap is reduced and gradient artefacts are decreased. The cables between the recording computer and the amplifier can be replaced with fibre optical cables so the artefacts arise from the magnetic fields and from the RFP are minimised (Ullsperger & Debener, 2010; Allen et al., 2000).

The obtained EEG data during simultaneous acquisition suffers from physiological and imaging artefacts, resulting in decreased data quality (Ives et al., 1993). There are two main artefacts that contaminate the EEG data, the (i) MR imaging-related gradient artefact and the (ii) pulse artefact (Niazy et al., 2005).

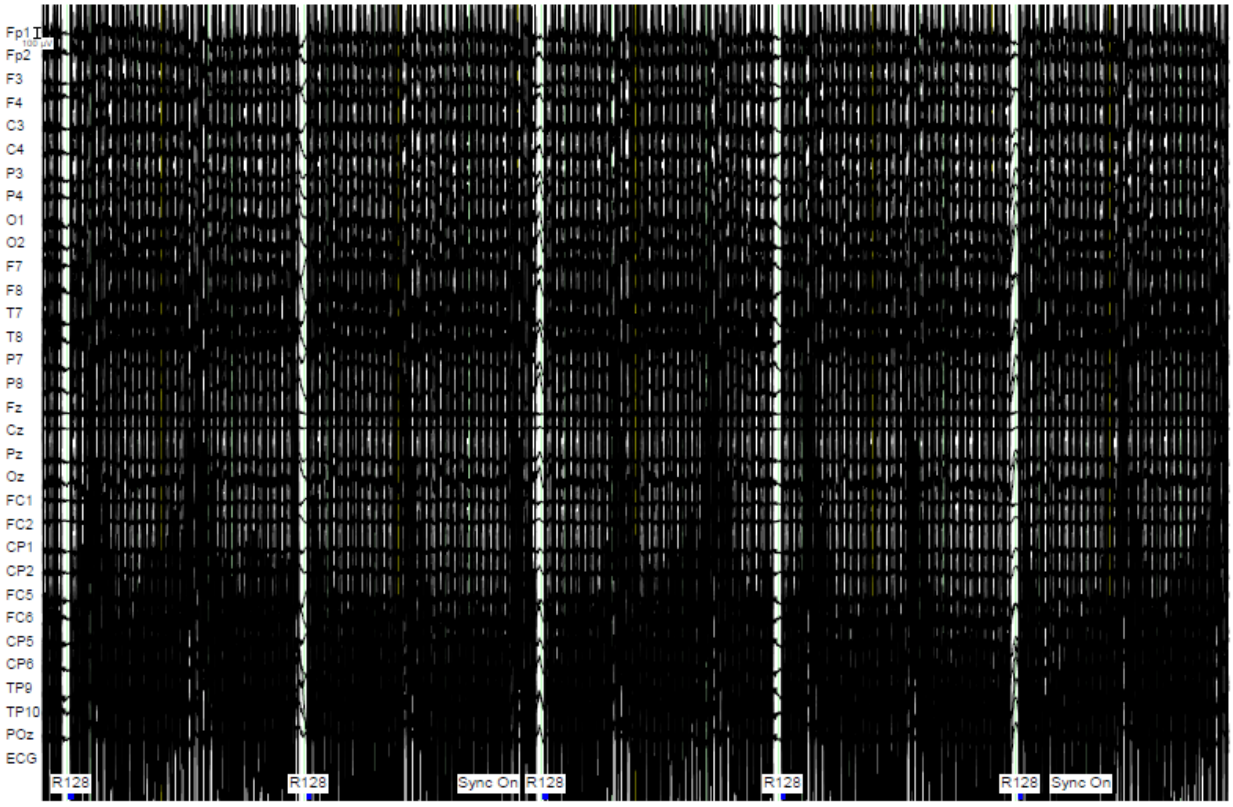

Figure 2. The raw EEG data from simultaneous EEG and fMRI acquisition. The pattern of the gradient artefacts is clearly visible on the EEG data; the artefact is covering the entire spectrum of EEG frequencies. Sync On sign shows the time of the clock synchronisation of the hardware. R128 is the trigger timing of the MR hardware clock, indicates the appearance of the GA. The EEG data is analysed and presented with BrainVision, Analyzer 2.2.

4. SOURCES OF ARTEFACTS ON THE EEG DATA DURING SIMULTAENOUS EEG and fMRI RECORDING

i. GRADIENT ARTEFACT - GA

GA is considered as an exogenous or technical artefact; gradient coils are essential for MRI data acquisition. This generates time-varying magnetic field changes during image acquisition and induces an electromotive force within the wire loop (Goldman et al., 2000). The amplitude of the induced voltage can be 100 times larger than the actual EEG signal. Yet, the EEG frequency bands of interest and GA frequency generally overlap, making the artefact correction more complicated. The waveform, the shape and the amplitude of GA can vary, depending on the location and the wire connection of the electrodes (Hoffman et al., 2000; Yan et al., 2009).

ii. PULSE ARTEFACT – PA

PA is known as one of the most challenging artefacts in simultaneous EEG and fMRI recording and is commonly referred to as ballistocardiogram artefact. The artefact possibly arises from the interaction of the cardiovascular system and the magnetic field although the exact origin is not known yet. PA is consistently present in the lower frequency band (< 15Hz) of the recorded signal on all electrode channels (Ullsperger & Debener, 2010; Mullinger et.al, 2013).

PA is characterised as a non-consistent, variant phenomenon as its appearance varies between participants and in single individuals which makes the identification and the process of the artefact correction significantly more difficult, relative to GA (Debener et al., 2008).

5. ARTEFACT CORRECTION: AVERAGE ARTEFACT TEMPLATE SUBTRACTION - AAS

i. GRADIENT ARTEFACT

There are several techniques available to reduce artefacts. A simple method is applying low-pass filtering although it is unlikely to be efficient as the induced voltages overlap with the band of the frequency of interests. Independent component Analysis (ICA) is a conventional correction approach; the data is decayed into independent components and each component is compared with the artefact template (Grouiller et al., 2007).

However, the invariant temporal occurrence and the well-known source of artefacts allowed to establish a more efficient artefact correction method. ASS is based on the subtraction of an average artefact template. The artefact template is obtained by averaging the occurred artefacts (intervals) across the data for each electrode. The calculated template for each electrode is then subtracted from the original data in the relevant intervals (Allen et al., 2000).

However, the efficiency of AAS highly depends on the precise temporal information of the onset of each GA and assumes that all the GA are obtained by the EEG amplifier. The accurate trigger timing can be ensured by the application of high frequency sample rate of 5000Hz and trigger marks to onset of GA. This could be achieved by the computer clocks synchronisation between EEG and fMRI (Hermann and Debener, 2008). Allen and colleagues suggested that AAS does not perfectly remove the artefacts therefore application of low-pass filter on the EEG data is recommended before further transformations (Allen et al., 2000).

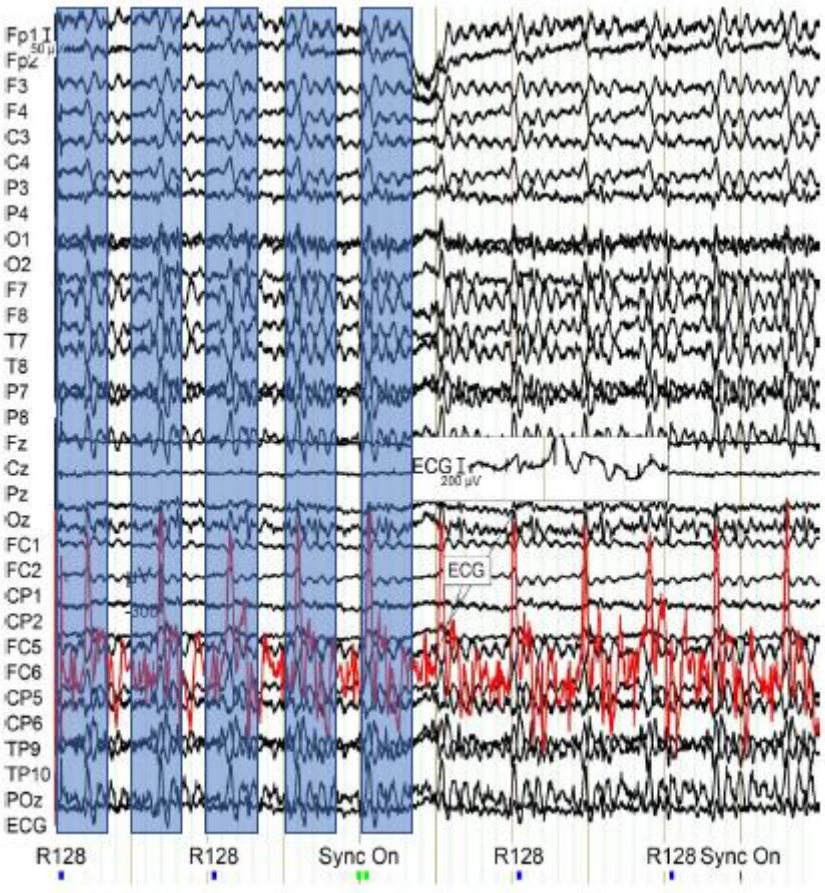

Figure 3. The GA corrected data. After the GA correction, PA (is highlighted with blue) is still present in the data. The occurrence of the artefact and the cardiac pulse are relatively correlate.

ii. PULSE ARTEFACT

The removal of PA is way more challenging than GA as the predictability of the artefact is minimised due to the high temporal variability and the multi-contributed sources of PA. Blood flow and B0 are fixed factors; the movements of the head and the electrodes in the scanner are limited therefore preventing the artefact formation on the first level is problematic. AAS is the most commonly used method for PA correction. The subtraction algorithm is based on the R-peak detection (from the QRS complex). First, an estimation of the onset of each cardiac cycle is applied; then, the algorithm creates an average PA waveform that contains couple of R-R intervals that are time-locked to the relevant R-peaks

for all EEG channels. The averaged waveform of the artefacts template is subtracted from the original data (Allen et al., 1998).

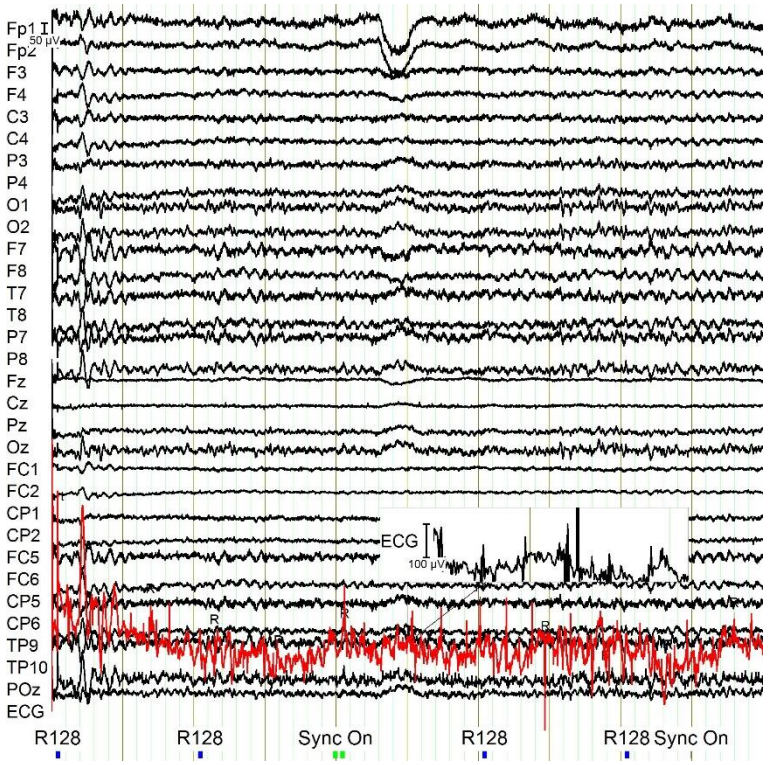

Figure 4. PA corrected data, the amplitudes of the PA are substantially reduced on all EEG channels means that the R peaks were successfully identified and resulting a clearer interpretation of the data.

REFERENCES

Allen, P. J., Polizzi, G., Krakow, K., Fish, D. R., & Lemieux, L. (1998). Identification of EEG events in the MR scanner: the problem of pulse artifact and a method for its subtraction. *Neuroimage*, *8*(3), 229-239.

Allen, P. J., Josephs, O., & Turner, R. (2000). A method for removing imaging artifact from continuous EEG recorded during functional MRI. *Neuroimage*, *12*(2), 230-239.

Babiloni, F., Mattia, D., Babiloni, C., Astolfi, L., Salinari, S., Basilisco, A., ... & Cincotti, F. (2004). Multimodal integration of EEG, MEG and fMRI data for the solution of the neuroimage puzzle. Magnetic resonance imaging, 22(10), 1471-1476.

Babiloni, C., Pizzella, V., Del Gratta, C., Ferretti, A., & Romani, G. L. (2009). Fundamentals of electroencefalography, magnetoencefalography, and functional magnetic resonance imaging. *International review of neurobiology*, *86*, 67-80.

Cohen, M. X. (2017). Where does EEG come from and what does it mean?. *Trends in neurosciences*, *40*(4), 208-218.

Currie, S., Hoggard, N., Craven, I. J., Hadjivassiliou, M., & Wilkinson, I. D. (2013). Understanding MRI: basic MR physics for physicians. *Postgraduate medical journal*, *89*(1050), 209-223.

Debener, S., Ullsperger, M., Siegel, M., & Engel, A. K. (2006). Single-trial EEG–fMRI reveals the dynamics of cognitive function. *Trends in cognitive sciences*, *10*(12), 558-563.

Debener, S., Mullinger, K. J., Niazy, R. K., & Bowtell, R. W. (2008). Properties of the ballistocardiogram artefact as revealed by EEG recordings at 1.5, 3 and 7 T static magnetic field strength. *International Journal of Psychophysiology*, *67*(3), 189-199.

Goldman, R. I., Stern, J. M., Engel Jr, J., & Cohen, M. S. (2002). Simultaneous EEG and fMRI of the alpha rhythm. *Neuroreport*, *13*(18), 2487.

Gotman, J., Kobayashi, E., Bagshaw, A. P., Bénar, C. G., & Dubeau, F. (2006). Combining EEG and fMRI: a multimodal tool for epilepsy research. *Journal of Magnetic Resonance Imaging: An Official Journal of the International Society for Magnetic Resonance in Medicine*, *23*(6), 906-920.

Grouiller, F., Vercueil, L., Krainik, A., Segebarth, C., Kahane, P., & David, O. (2007). A comparative study of different artefact removal algorithms for EEG signals acquired during functional MRI. *Neuroimage*, *38*(1), 124-137.

Herrmann, C. S., & Debener, S. (2008). Simultaneous recording of EEG and BOLD responses: a historical perspective. *International Journal of Psychophysiology*, *67*(3), 161-168.

Hoffmann, A., Jäger, L., Werhahn, K. J., Jaschke, M., Noachtar, S., & Reiser, M. (2000). Electroencephalography during functional echo-planar imaging: detection of epileptic spikes using post-processing methods. *Magnetic Resonance in Medicine: An Official Journal of the International Society for Magnetic Resonance in Medicine*, *44*(5), 791-798.

Ives, J. R., Warach, S., Schmitt, F., Edelman, R. R., & Schomer, D. L. (1993). Monitoring the patient's EEG during echo planar MRI. *Electroencephalography and clinical neurophysiology*, *87*(6), 417-420.

Mayhew, S. D., & Bagshaw, A. P. (2017). Dynamic spatiotemporal variability of alpha-BOLD relationships during the resting-state and task-evoked responses. *NeuroImage*, *155*, 120-137.

Murbach, M., Zastrow, E., Neufeld, E., Cabot, E., Kainz, W., & Kuster, N. (2015). Heating and safety concerns of the radio-frequency field in MRI. *Current Radiology Reports*, *3*(12), 45.

Laufs, H., Daunizeau, J., Carmichael, D. W., & Kleinschmidt, A. (2008). Recent advances in recording electrophysiological data simultaneously with magnetic resonance imaging. *Neuroimage*, *40*(2), 515-528.

Lemieux, L., Allen, P. J., Franconi, F., Symms, M. R., & Fish, D. K. (1997). Recording of EEG during fMRI experiments: patient safety. *Magnetic Resonance in Medicine*, *38*(6), 943-952.

Logothetis, N. K. (2002). The neural basis of the blood–oxygen–level–dependent functional magnetic resonance imaging signal. *Philosophical Transactions of the Royal Society of London. Series B: Biological Sciences*, *357*(1424), 1003-1037.

Logothetis, N. K. (2008). What we can do and what we cannot do with fMRI. *Nature*, *453*(7197), 869.

Makeig, S., Delorme, A., Westerfield, M., Jung, T. P., Townsend, J., Courchesne, E., & Sejnowski, T. J. (2004). Electroencephalographic brain dynamics following manually responded visual targets. *PLoS biology*, *2*(6), e176.

Mele, G., Cavaliere, C., Alfano, V., Orsini, M., Salvatore, M., & Aiello, M. (2019). Simultaneous EEG-fMRI for functional neurological assessment. *Frontiers in neurology*, *10*, 848.

Mullinger, K. J., Havenhand, J., & Bowtell, R. (2013). Identifying the sources of the pulse artefact in EEG recordings made inside an MR scanner. *Neuroimage*, *71*, 75-83.

Niazy, R. K., Beckmann, C. F., Iannetti, G. D., Brady, J. M., & Smith, S. M. (2005). Removal of FMRI environment artifacts from EEG data using optimal basis sets. *Neuroimage*, *28*(3), 720-737.

Ogawa, S., Lee, T. M., Nayak, A. S., & Glynn, P. (1990). Oxygenation-sensitive contrast in magnetic resonance image of rodent brain at high magnetic fields. *Magnetic resonance in medicine*, *14*(1), 68-78.

Ruff, C. C., & Huettel, S. A. (2014). Experimental methods in cognitive neuroscience. In *Neuroeconomics* (pp. 77-108). Academic Press.

Uji, M., Wilson, R., Francis, S. T., Mullinger, K. J., & Mayhew, S. D. (2018). Exploring the advantages of multiband fMRI with simultaneous EEG to investigate coupling between gamma frequency neural activity and the BOLD response in humans. *Human brain mapping*, *39*(4), 1673-1687.

Ullsperger, M., & Debener, S. (2010). *Simultaneous EEG and fMRI: recording, analysis, and application*. Oxford University Press.

Teplan, M. (2002). Fundamentals of EEG measurement. *Measurement science review*, *2*(2), 1-11.

Yan, W. X., Mullinger, K. J., Brookes, M. J., & Bowtell, R. (2009). Understanding gradient artefacts in simultaneous EEG/fMRI. *Neuroimage*, *46*(2), 459-471.

APPENDIX 1

Specific Absorption Rate: SAR is described as the radiofrequency (RF) power absorbed per unit of mass of a tissue and measured in watts per kilogram (W/kg). Due to the inhomogeneity of the radio-frequency field the absorbed energy expends in local body region (local SAR) and can be averaged over the whole body (global SAR). To prevent any complications, the frequency and the power of the radio frequency irradiation should be maintained at the lowest possible level (Murbach et al., 2015).

To investigate the energy explosion of SAR on the electrodes, we have acquired simultaneous EEG and fMRI while high sensitivity heating fibre optical sensors were placed to 3 different EEG electrodes (Cz, T7, ECG) on a phantom and the main magnet bore. Figure 1. presents the fluctuations of the measured temperatures during different type of anatomical or functional scans. According to IEC 60601-2-33 (2002), the local temperature alterations should not be more than 1°C regards to the considered safe limit for EEG heating. Some of the measured temperature differences were relatively close or over the limit. The TSE scans reached the safety limit by increasing plus 1.25 °C on the ECG electrode, the HCP functional scan show relatively large increase on Cz electrode. The inconsistency of the electrode location of the temperature increases have not been clarified yet, further investigation is arranged. The collected data is acquired during one session therefore the interpretation of the results could not provide solid conclusions; the repetition of the experiment is recommended.